

# Renormalization group approach to energy level statistics at the integer quantum Hall transition

Philipp Cain and Rudolf A. Römer\*

*Institut für Physik, Technische Universität Chemnitz, D-09107 Chemnitz, Germany*

Mikhail E. Raikh

*Department of Physics, University of Utah, Salt Lake City, Utah 84112*

(Dated: *Revision* : 1.24, compiled October 27, 2018)

We extend the real-space renormalization group (RG) approach to the study of the energy level statistics at the integer quantum Hall (QH) transition. Previously it was demonstrated that the RG approach reproduces the critical distribution of the *power* transmission coefficients, i.e., two-terminal conductances,  $P_c(G)$ , with very high accuracy. The RG flow of  $P(G)$  at energies away from the transition yielded the value of the critical exponent,  $\nu$ , that agreed with most accurate large-size lattice simulations. To obtain the information about the level statistics from the RG approach, we analyze the evolution of the distribution of *phases* of the *amplitude* transmission coefficient upon a step of the RG transformation. From the fixed point of this transformation we extract the critical level spacing distribution (LSD). This distribution is close, but distinctively different from the earlier large-scale simulations. We find that away from the transition the LSD crosses over towards the Poisson distribution. Studying the change of the LSD around the QH transition, we check that it indeed obeys scaling behavior. This enables us to use the alternative approach to extracting the critical exponent, based on the LSD, and to find  $\nu = 2.37 \pm 0.02$  very close to the value established in the literature. This provides additional evidence for the surprising fact that a small RG unit, containing only five nodes, accurately captures most of the correlations responsible for the localization-delocalization transition.

PACS numbers: 73.43.-f, 73.43.Nq, 64.60.Ak

## I. INTRODUCTION

It has been realized long ago that, alongside with the change in the behavior of the eigenfunctions, a localization-delocalization transition manifests itself in the statistics of the energy levels. In particular, as the energy is swept across the mobility edge, the shape of the level spacing distribution (LSD) crosses over from the Wigner-Dyson distribution, corresponding to the appropriate universality class, to the Poisson distribution.

Moreover, finite-size corrections to the critical LSD exactly at the mobility edge allow to determine the value of the correlation length exponent,<sup>1</sup> thus avoiding an actual analysis of the spatial extent of the wave functions. For this reason, the energy level statistics constitutes an alternative to the MacKinnon-Kramer<sup>2,3,4,5</sup> and to the transmission-matrix<sup>6,7</sup> approaches to the numerical study of localization.

Another reason why a large number of numerical simulations of the LSD at the transition<sup>8,9,10,11,12,13,14,15,16,17,18,19,20,21,22</sup> were carried out during the past decade is the controversy that existed over the large-spacing tail of the critical LSD. Conclusive demonstration<sup>12,13,21</sup> that this tail is Poissonian, i.e., that there is no repulsion between the levels with spacings much larger than the mean value,<sup>1</sup> rather than super-Poissonian,<sup>23</sup> implying that repulsion is partially preserved, required a very high accuracy of the simulations.<sup>13,21</sup> The bulk of numerical work on the level statistics at the transition was carried out

for three-dimensional systems<sup>8,9,10,11,12,13,14</sup> for which there exists a mobility edge separating localized and extended states. In two dimensions all the states are localized in the absence of a magnetic field. In the presence of a magnetic field, localization-delocalization transitions in two dimensions (quantum Hall transitions) are infinitely sharp. Still the reasoning of Ref. 1 applies. Numerical studies have established a Poissonian tail of the LSD.<sup>19</sup> It was also demonstrated<sup>19</sup> that the procedure of extracting the localization length exponent from the finite-size corrections yields a value close to  $\nu = 2.35$  found from large-size simulations of the wave functions.<sup>24,25,26,27</sup>

Recently, a semianalytical description of the integer quantum Hall transition, based on the extension of the scaling ideas for the classical percolation<sup>28</sup> to the Chalker-Coddington (CC) model of the quantum percolation,<sup>29</sup> has been developed.<sup>30,31</sup> The key idea of this description, a real-space-renormalization group approach (RG), is the following. Each RG step corresponds to a doubling of the system size. The RG transformation relates the conductance *distribution* of the sample at the next step to the conductance distribution at the previous step. The *fixed point* of this transformation, yields the distribution of the conductance,  $P_c(G)$  of a *macroscopic* sample at the quantum Hall transition. This *universal* distribution describes the mesoscopic properties of a fully coherent quantum Hall sample. Analogously to the classical percolation,<sup>28</sup> the correlation length exponent,  $\nu$ , was extracted from the RG procedure<sup>32</sup> using the fact that a slight shift of the initial distribution with respect

to the fixed-point,  $P_c(G)$ , drives the system to the insulator upon renormalization. Then the rate of the shift of the distribution maximum determines the value of  $\nu$ . Remarkably, both  $P_c(G)$  and the critical exponent obtained within the RG approach<sup>32,33,34</sup> agree very well with the “exact” results of the large-scale simulations.<sup>25,27,35,36,37</sup>

The goal of the present paper is two-fold. Firstly, we extend the RG approach to the level statistics at the transition in order to subject its validity to yet another test. Secondly, we apply the method analogous to the finite-size-corrections analysis to extract  $\nu$  from the LSD obtained within the RG approach. This method yields  $\nu = 2.37 \pm 0.02$ , which is even closer to the most precise large-scale simulations result  $\nu = 2.35 \pm 0.03$ <sup>25</sup> than the value  $\nu = 2.39 \pm 0.01$  inferred from the conductance distribution.<sup>32</sup> The latter result is by no means trivial. Indeed, the original RG transformation<sup>32</sup> related the conductances, i.e., the *absolute values* of the transmission coefficients of the original and the doubled samples, while the *phases* of the transmission coefficients were assumed random and uncorrelated. In contrast, the level statistics at the transition corresponds to the fixed point in the distribution of these phases. Therefore, the success of the RG approach for conductances does not guarantee that it will be equally accurate *quantitatively* for the level statistics.

Within both RG transformations, for the magnitudes and for the phases of the transmission coefficients, an initial deviation from the critical distribution drives the system towards an insulator with zero transmission and Poissonian LSD. Thus the procedures of the extraction of  $\nu$  from both transformations are technically different, but conceptually similar. In fact, the shape of the critical LSD, obtained from the RG approach, shows systematic deviations from the large-scale simulation results<sup>17,18,19,20,21,22,38,39</sup> which yield the body of LSD very close to the Gaussian unitary random matrix ensemble (GUE).<sup>40</sup> However, the RG flow of the LSD towards the insulator appears to be robust.

The paper is organized as follows. First, in Sec. II we review the real-space RG approach<sup>30,31,32</sup> and adjust it to the computation of the energy levels and the LSD. In Sec. III we present our numerical results for the LSD. The finite-size scaling (FSS) analysis of the obtained LSD at the QH transition is reported in Sec. IV. Concluding remarks are presented in Sec. V.

## II. MODEL AND RG METHOD FOR THE LSD

### A. RG approach to the conductance distribution

A detailed description of the RG approach to the conductance distribution can be found in Refs. 30,31,32. It is

based on the RG unit shown in Fig. 1. The unit is a fragment of the CC network consisting of five nodes. Each node,  $i$ , is characterized by the transmission coefficient  $t_i$ , which is an amplitude to deflect an incoming electron

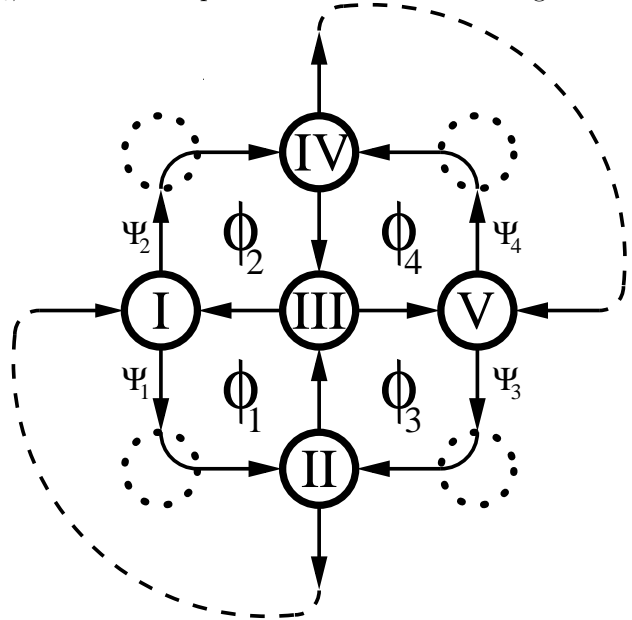


FIG. 1: Chalker-Coddington network on a square lattice consisting of nodes (circles) and links (arrows). The RG unit used for Eq. (1) combines five nodes (full circles) by neglecting some connectivity (dashed circles).  $\Phi_1, \dots, \Phi_4$  are the phases acquired by an electron along the loops as indicated by the arrows.  $\Psi_1, \dots, \Psi_4$  represent wave function amplitudes, and the thin dashed lines illustrate the boundary conditions used for the computation of level statistics.

along the link to the left. Analogously, the reflection coefficient  $r_i = (1 - t_i^2)^{1/2}$  is the amplitude to deflect the incoming electron to the right. Doubling of the sample size corresponds to the replacement of the RG unit by a single node. The RG transformation expresses the transmission coefficient of this effective node,  $t'$ , through the transmission coefficients of the five constituting nodes<sup>30</sup>

$$t' = \left| \frac{t_1 t_5 (r_2 r_3 r_4 e^{i\Phi_2} - 1) + t_2 t_4 e^{i(\Phi_3 + \Phi_4)} (r_1 r_3 r_5 e^{-i\Phi_1} - 1) + t_3 (t_2 t_5 e^{i\Phi_3} + t_1 t_4 e^{i\Phi_4})}{(r_3 - r_2 r_4 e^{i\Phi_2})(r_3 - r_1 r_5 e^{i\Phi_1}) + (t_3 - t_4 t_5 e^{i\Phi_4})(t_3 - t_1 t_2 e^{i\Phi_3})} \right|. \quad (1)$$

Here  $\Phi_j$  are the phases accumulated along the closed loops (see Fig. 1). Within the RG approach to the conductance distribution, information about electron energy is incorporated only into the values of  $t_i$ . The energy dependence of phases,  $\Phi_j$ , is irrelevant; they are assumed completely random. Due to this randomness, the transmission coefficients,  $t_i$ , for a given energy, are also randomly distributed with a distribution function  $P(t)$ . Then the transformation (1) allows, upon averaging over  $\Phi_j$ , to generate the next-step distribution  $P(t')$ . Therefore, within the RG scheme, a delocalized state corresponds to the fixed point,  $P_c(t)$ , of the RG transformation. Due to the symmetry of the RG unit, it is obvious that the critical distribution,  $P_c(t^2)$ , of the power transmission coefficient,  $t^2 = G$ , which has the meaning of the two-terminal conductance, is symmetric with respect to  $t^2 = \frac{1}{2}$ . In other words, the RG transformation respects the duality between transmission and reflection. The critical distribution  $P_c(G)$  found in Refs. 30 and 32 agrees very well with the results of direct large-scale simulations.

## B. RG approach to the LSD

Universal features of the energy level statistics in a macroscopic fully coherent sample at the quantum Hall

transition complement the universality in the conductance distribution. The prime characteristics of the level statistics is the LSD – the distribution of the spacings between neighboring energy levels. In order to adjust the RG approach to the calculation of the LSD, it is necessary to “close” the sample at each RG step in order to discretize the energy levels. One of the possible variants of such a closing is shown in Fig. 1 with dashed lines.

For a given closed RG unit with a fixed set of  $t_i$ -values at the nodes, the positions of the energy levels are determined by the energy dependences,  $\Phi_j(E)$ , of the four phases along the loops. These phases change by  $\sim \pi$  within a very narrow energy interval, inversely proportional to the sample size. Within this interval the change of the transmission coefficients is negligibly small. A closed RG unit in Fig. 1 contains 10 links, and, thus, it is described by 10 amplitudes. These amplitudes are related by 10 equations (2 at each node). Each link is characterized by an individual phase. On the other hand, it is obvious that the energy levels are determined only by the phases along the loops. One possible way to derive the system, in which individual phases combine into  $\Phi_j$  is to exclude from the original system of 10 equations all amplitudes except the “boundary” amplitudes  $\Psi_j$  (see Fig. 1). This procedure is similar to the derivation of Eq. (1). The system of equations for the remaining four amplitudes takes the form

$$\begin{pmatrix} (r_1 r_2 - t_1 t_2 t_3) e^{-i\Phi_1} & (t_1 r_2 + t_2 t_3 r_1) e^{-i\Phi_1} & t_2 t_5 r_3 e^{-i\Phi_1} & t_2 r_3 r_5 e^{-i\Phi_1} \\ -t_1 r_3 r_4 e^{-i\Phi_2} & r_1 r_3 r_4 e^{-i\Phi_2} & -(t_4 r_5 + t_3 t_5 r_4) e^{-i\Phi_2} & (t_4 t_5 - t_3 r_4 r_5) e^{-i\Phi_2} \\ -t_1 t_4 r_3 e^{-i\Phi_4} & t_4 r_1 r_3 e^{-i\Phi_4} & (r_4 r_5 - t_3 t_4 t_5) e^{-i\Phi_4} & -(t_5 r_4 + t_3 t_4 r_5) e^{-i\Phi_4} \\ -(t_2 r_1 + t_1 t_3 r_2) e^{-i\Phi_3} & -(t_1 t_2 - t_3 r_1 r_2) e^{-i\Phi_3} & t_5 r_2 r_3 e^{-i\Phi_3} & r_2 r_3 r_5 e^{-i\Phi_3} \end{pmatrix} \begin{pmatrix} \Psi_1 \\ \Psi_2 \\ \Psi_3 \\ \Psi_4 \end{pmatrix} = e^{i\omega} \begin{pmatrix} \Psi_1 \\ \Psi_2 \\ \Psi_3 \\ \Psi_4 \end{pmatrix}, \quad (2)$$

where the parameter  $\omega$  should be set zero. Then the energy levels,  $E_k$ , of the closed RG unit are the energies for which, with phases  $\Phi_j(E) = \Phi_j(E_k)$ , one of the four eigenvalues of the matrix in the left-hand side of Eq. (2) is equal to one. If we keep  $\omega$  in the right-hand side of Eq. (2), then the above condition can be reformulated as  $\omega(E_k) = 0$ . Thus, the calculation of the energy levels reduces to a diagonalization of the  $4 \times 4$  matrix.

The crucial step now is the choice of the dependence  $\Phi_j(E)$ . If each loop in Fig. 1 is viewed as a closed equipotential as it is the case for the first step of the RG procedure,<sup>29</sup> then  $\Phi_j(E)$  is a true magnetic phase, which changes linearly with energy with a slope governed by

the actual potential profile, which, in turn, determines the drift velocity. Thus we have

$$\Phi_j(E) = \Phi_{0,j} + 2\pi \frac{E}{s_j}, \quad (3)$$

where a random part,  $\Phi_{0,j}$ , is uniformly distributed within  $[0, 2\pi]$ , and  $2\pi/s_j$  is a random slope. Strictly speaking, the dependence (3) applies only for the first RG step. At each following step,  $n > 1$ ,  $\Phi_j(E)$  is a complicated function of  $E$  which carries information about all energy scales at previous steps. However, in the spirit of the RG approach, we assume that  $\Phi_j(E)$  can still be linearized within a relevant energy interval. The conven-

tional RG approach suggests that different scales in the *real* space can be decoupled. Linearization of Eq. (3) implies a similar decoupling in the *energy* space. In the case of phases, a “justification” of such a decoupling is that at each following RG step, the relevant energy scale, that is the mean level spacing, reduces by a factor of 4.

With  $\Phi_j(E)$  given by Eq. (3) and fixed values of  $t_i$ , the statistics of energy levels determined by the matrix equation (2) is obtained by averaging over the random initial phases  $\Phi_{0,j}$ . In particular, each realization of  $\Phi_{0,j}$  yields 3 level spacings which are then used to construct a smooth LSD. We now outline the RG procedure for the LSD. The slopes  $s_j$  in Eq. (3) determine the level spacings at the first step. They are randomly distributed with a distribution function  $P_0(s)$ . Diagonalization of the matrix in Eq. (2) with subsequent averaging over realizations yields the LSD,  $P_1(s)$ , at the second step. Then the key element of the RG procedure, as applied to the level statistics, is using  $P_1(s)$  as a *distribution of slopes* in Eq. (3). This leads to the next-step LSD and so on.

It is instructive to compare our procedure of calculating the energy levels with an approach adopted in large-scale simulations within the CC model.<sup>14,39</sup> This approach is based on the unitary network operator  $U$ .<sup>39</sup> For a single RG unit this operator acts analogously to the matrix in the left-hand side of Eq. (2). However, within the approach of Refs. 14 and 39, the energy dependence of phases  $\Phi_j$  in the elements of the matrix was neglected (only the random contributions,  $\Phi_{0,j}$ , were kept). Then, instead of the energy levels,  $E_k$ , diagonalization of the matrix (2) yielded a set of eigenvalues,  $\exp(i\omega_k)$ . The numbers  $\omega_k$  were named *quasienergies*, and it is the statistics of these quasienergies that was studied in Ref. 39. Comparison of the two procedures for a single RG unit is illustrated in Fig. 2. Fig. 2 shows the dependence of the 4 quasienergies  $\omega_k$  on the energy  $E$  calculated for two single sample RG units, with  $t_i$  chosen from the critical distribution  $P_c(t)$ . The energy dependence of the phases  $\Phi_j$  was chosen from LSD of the GUE according to Eq. (3). It is seen that the dependences  $\omega(E)$  range from remarkably linear and almost parallel (Fig. 2a) to strongly nonlinear (Fig. 2b).

### III. NUMERICAL RESULTS

#### A. The LSD at the QH transition

As a first step of the RG procedure for the calculation of the critical LSD we chose for  $P_0(s)$  the distribution corresponding to the GUE random matrix ensemble, since previous simulations<sup>19,39</sup> indicated that the LSD at the transition is close to GUE. According to  $P_0(s)$ , we pick  $s_j$  and set  $\Phi_j$ ,  $j = 1, \dots, 4$  as in Eq. (3). For the transmission coefficients  $t_i$ ,  $i = 1, \dots, 5$  we use the fixed-point distribution  $P_c(t)$ ,<sup>41</sup> obtained previously.<sup>32</sup>

From the solutions of Eq. (2) corresponding to  $\omega_j(E_k) = 0$  the new LSD  $P_1(s')$  is constructed using the

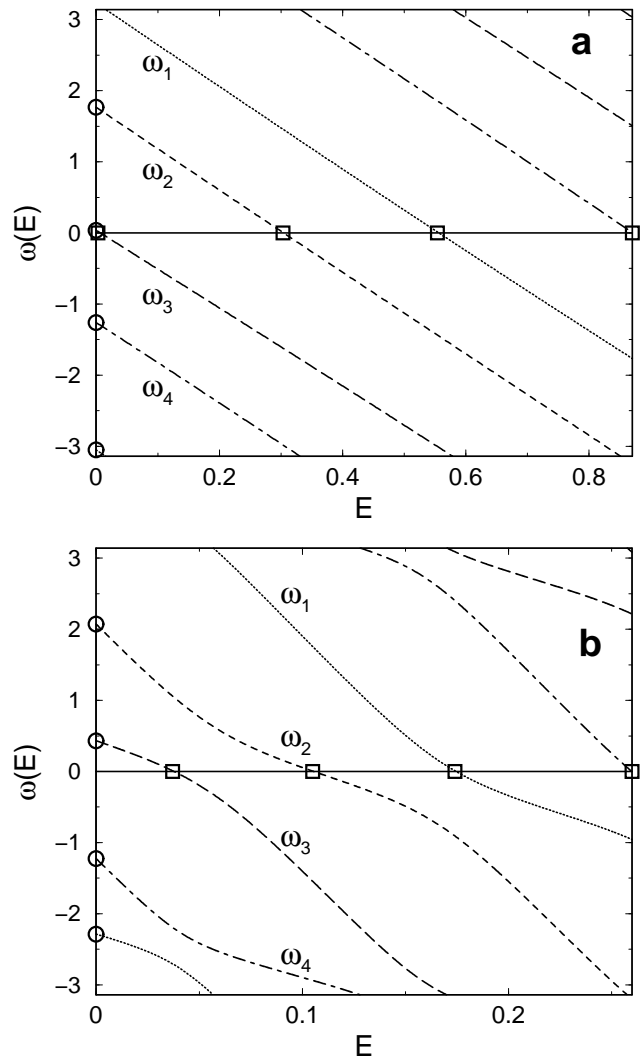


FIG. 2: Energy dependence of the quasienergies  $\omega$  for two sample configurations. Instead of using the quasispectrum obtained from  $\omega_l(E = 0)$  ( $\circ$ ) we calculate the real eigenenergies according to  $\omega(E_k) = 0$  ( $\square$ ). Different line styles distinguish different  $\omega_l(E)$ . We emphasize that the observed behavior varies from sample to sample between remarkably linear (a) and strongly nonlinear (b).

“unfolded” energy level spacings  $s'_m = (E_{m+1} - E_m)/\Delta$ , where  $m = 1, 2, 3$ ,  $E_{k+1} > E_k$  and the mean spacing  $\Delta = (E_4 - E_1)/3$ . Due to the “unfolding”<sup>42</sup> with  $\Delta$ , the average spacing is set to one for each sample and in each RG-iteration step we superimpose spacing data of  $2 \times 10^6$  RG units. The resulting LSD is discretized in bins with largest width 0.01. In the following iteration step we repeat the procedure using  $P_1$  as initial distribution. We assume that the iteration process has converged when the mean-square deviation of distribution  $P_n(s)$  deviates by less than  $10^{-4}$  from its predecessor  $P_{n-1}(s)$ . The RG iteration process converges rather quickly after only 2 – 3 RG steps. The resulting LSD,  $P_c(s)$ , is shown in Fig. 3 together with an LSD for the unitary random matrix

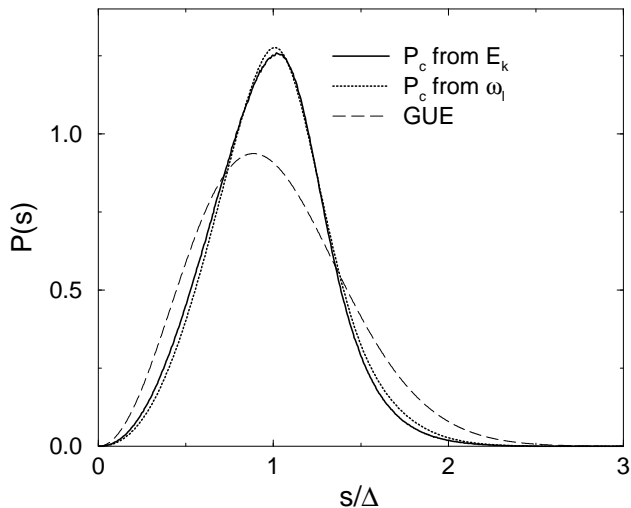


FIG. 3: Critical distributions  $P_c(s)$  obtained from the spectrum of  $\omega_l(E=0)$  and from the RG approach using the real eigenenergies  $E_k$  in comparison to the LSD for GUE. As in all other graphs  $P(s)$  is shown in units of the mean level spacing  $\Delta$ .

ensemble.

Although  $P_c(s)$  exhibits the expected features, namely, level repulsion for small  $s$  and a long tail at large  $s$ , the overall shape of  $P_c(s)$  differs noticeably from GUE. In the previous large-size lattice simulations<sup>19,39</sup> the obtained critical LSD was much closer to GUE than  $P_c(s)$  in Fig. 3. This fact, however, does not reflect on the accuracy of the RG approach. Indeed, as it was demonstrated recently, the critical LSD – although being system size independent – nevertheless depends on the geometry of the samples<sup>43</sup> and on the specific choice of boundary conditions.<sup>44,45</sup> Sensitivity to the boundary conditions does not affect the asymptotics of the critical distribution, but rather manifests itself in the shape of the “body” of the LSD. Recall now that the boundary conditions which we have imposed to calculate the energy levels (dashed lines in Fig. 1) are *non-periodic*.

There is another possibility to assess the critical LSD, namely by iterating the distribution of *quasienergies*. In Fig. 3 we show the result of this procedure. It appears that the resulting distribution is almost *identical* to  $P_c(s)$ . This observation is highly non-trivial, since, as follows from Fig. 2, there is no simple relation between the energies and quasienergies. Moreover, if instead of the linear  $E$ -dependence of  $\Phi_j$ , we choose another functional form, say,

$$\Phi_j(E) = \Phi_{0,j} + 2 \arcsin \left( \frac{E}{s_j} - 2p \right), \quad (4)$$

where the integer  $p$  insures that  $\left| \frac{E}{s_j} - 2p \right| \leq 1$ , then, the RG procedure would yield an LSD which is markedly different (within the “body”) from  $P_c(s)$ . This is illustrated in Fig. 4.

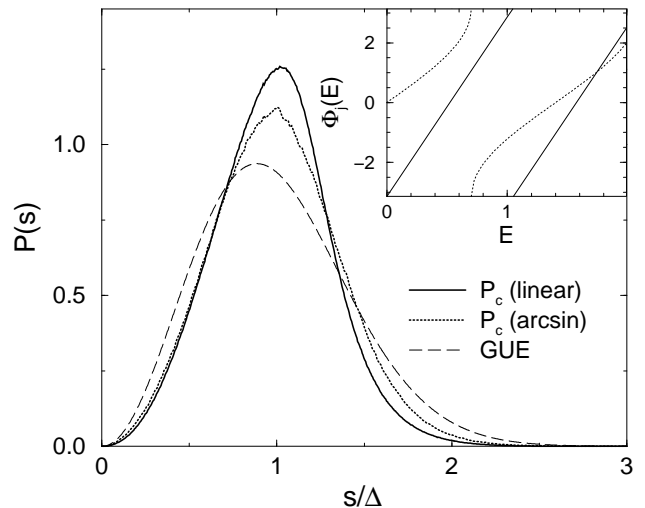


FIG. 4: Critical distributions  $P_c(s)$  for a linear and an arcsin energy dependence of the phases  $\Phi_j$ . The form of  $P_c(s)$  is clearly influenced by the actual choice of  $\Phi_j(E)$ . Hence the bulk of the distribution is non-universal. The inset illustrates examples of the two different functions  $\Phi_j(E)$  as in Eqs. (3) and (4).

Both procedures, using quasienergies instead of real energies [as in Ref. 39], and linearization of the energy dependence of phases [as in Eq. (3)] are not rigorous. Linearization is dictated by the RG concept. The coincidence of the results of the two procedures indicates that the concept of quasienergies, namely, that they obey the same statistics as real energies, is equivalent to the RG.

## B. Small and large $s$ behavior

As it was mentioned above, the general shape of the critical LSD is not universal. However, the small  $s$  behavior of  $P_c(s)$  must be the same as for the unitary random matrix ensemble, namely  $P_c(s) \propto s^2$ . This is because delocalization at the quantum Hall transition implies the level repulsion.<sup>1,46</sup> Earlier large-scale simulations of the critical LSD<sup>11,12,14,17,18,19,20,21,22,38,39</sup> satisfy this general requirement. The same holds also for our result, as can be seen in Fig. 5. The given error bars of our numerical data are standard deviations computed from a statistical average of 100 FP distributions each obtained for different random sets of  $t_i$ 's and  $\Phi_j$ 's within the RG unit. In general, within the RG approach, the  $s^2$ -asymptotics of  $P(s)$  is most natural. This is because the levels are found from diagonalization of the  $4 \times 4$  unitary matrix with absolute values of elements widely distributed between 0 and 1.

The right form of the large- $s$  tail of  $P(s)$  is Poissonian,  $P_c(s) \propto \exp(-bs)$ .<sup>1</sup> For the Anderson model in three dimensions, unambiguous confirmation of this prediction in numerical simulations became possible only when very high numerical accuracy had been achieved.<sup>12,13</sup> This is

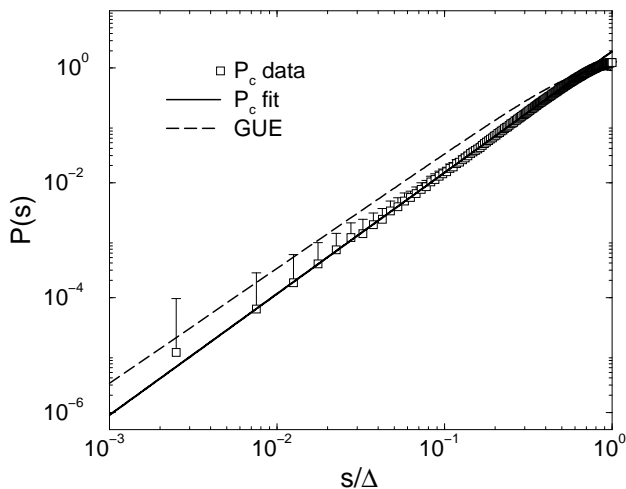


FIG. 5: Critical  $P_c(s)$  for small  $s$  in agreement with the predicted  $s^2$  behavior. Due to the log-log plot errors are shown in the upper direction only.

because  $P_c(s)$  assumes the Poissonian asymptotics only at large enough  $s \gtrsim 3\Delta$ . For the quantum Hall transition, a linear behavior of  $\ln P_c(s)$  with a slope corresponding to the value  $b \approx 4.1$  has been found in Ref. 19 from the analysis of the interval  $2 < s/\Delta < 4$ . Our data, as shown in Fig. 6, has a high accuracy only for  $s/\Delta \lesssim 2.5$ . For such  $s$ , the distribution  $P_c(s)$  does not yet reach its large- $s$  tail. Thus, the value of parameter  $b$  extracted from this limited interval is somewhat ambiguous. Namely, we obtain  $b = 5.442$  for  $s/\Delta \in [1.5, 2.0]$  and  $b = 6.803$  for  $s/\Delta \in [2.0, 2.5]$ .

Summarizing, the accuracy of the RG approach, applied to the level statistics, is insufficient to discern the only non-trivial feature of the critical LSD, i.e., the universal Poissonian asymptotics. However, the scaling analysis of LSD clearly reveals the universal features of the quantum Hall transition as we demonstrate in the next Section.

#### IV. SCALING RESULTS FOR THE LSD

##### A. Finite-size scaling at the QH transition

The critical exponent,  $\nu$ , of the quantum Hall transition governs the divergence of the correlation length  $\xi_\infty$  as a function of the arbitrary control parameter  $z_0$ , i.e.,

$$\xi_\infty(z_0) \propto |z_0 - z_c|^{-\nu}, \quad (5)$$

where  $z_c$  is the critical value. The values of  $\nu$  calculated using different numerical methods, e.g.,  $\nu = 2.35 \pm 0.03$ ,<sup>25</sup>  $2.4 \pm 0.2$ ,<sup>27</sup>  $2.5 \pm 0.5$ <sup>29</sup> agree with each other. The RG approach for the conductance distribution also yields a rather accurate value  $\nu = 2.39 \pm 0.01$ .<sup>32</sup> In Sec. II we have introduced a complimentary RG approach to the distribution of the energy levels at the transition. It can

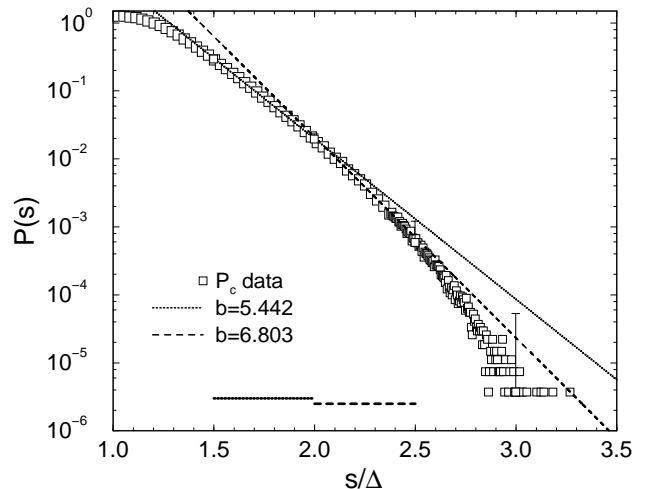


FIG. 6: The large  $s$  tail of  $P_c(s)$  compared with fits according to the predictions of Ref. 1 (lines). The interval used for fitting is indicated by the bars close to the lower axis. For clarity errors are shown in upper direction and for  $s/\Delta = 1.5, 2.0, 2.5, 3.0$  only. For  $s/\Delta < 2.4$ , only every 5th data point is drawn by a symbol.

be expected on general grounds, that the LSD obtained from the RG approach obeys scaling at small enough  $z_0 - z_c$ . However, it is by now means obvious, whether the value of  $\nu$  extracted from different variants of the RG approach are consistent.

In order to extract  $\nu$  from the LSD we employ the one-parameter-scaling analysis. This analysis is based on the rescaling of a quantity  $\alpha(N; \{z_i\})$  — depending on (external) system parameters  $\{z_i\}$  and the system size  $N$  — onto a single curve by using a scaling function  $f$

$$\alpha(N; \{z_i\}) = f\left(\frac{N}{\xi_\infty(\{z_i\})}\right). \quad (6)$$

Since Eq. (5), as indicated by “ $\infty$ ”, holds only in the limit of infinite system size, we now use the scaling assumption to extrapolate  $f$  to  $N \rightarrow \infty$  from the finite-size results of the computations. Once  $f$  and  $\xi_\infty$  are known, the value of  $\nu$  can be then inferred.

In the original formulation of the RG approach<sup>30</sup> it was demonstrated that there is a natural parametrization of the transmission coefficients  $t$ , i.e.,  $t = (e^z + 1)^{-1/2}$ . For such a parametrization,  $z$  can be identified with a dimensionless electron energy. The quantum Hall transition occurs at  $z = 0$ , which corresponds to the center of the Landau band. The universal conductance distribution at the transition,  $P_c(G)$ , corresponds to the distribution  $Q_c(z) = P_c[(e^z + 1)^{-1}] / 4 \cosh^2(z/2)$  of parameter  $z$ , which is symmetric with respect to  $z = 0$  and has a shape close to a gaussian.<sup>32</sup> The RG procedure for the conductance distribution converges and yields  $Q_c(z)$  only if the initial distribution is an even function of  $z$ . This suggests to choose as a control parameter in Eq. (6),  $z_0$ , the position of the maximum of the function  $Q(z)$ . Then

the meaning of  $z_0$  is the electron energy measured from the center of Landau band. The fact that the quantum Hall transition is infinitely sharp implies that for any  $z_0 \neq 0$ , the RG procedure drives the initial distribution  $Q(z - z_0)$  towards an insulator, either with complete transmission of the network nodes (for  $z_0 > 0$ ) or with complete reflection of the nodes (for  $z_0 < 0$ ).

### B. Scaling for $\alpha_P$ and $\alpha_I$

In principle, we are free to choose for the finite-size analysis any characteristic quantity  $\alpha(N; z_0)$  constructed from the LSD which has a systematic dependence on system size  $N$  for  $z_0 \neq 0$  while being constant at the transition  $z_0 = 0$ . Because of the large number of possible choices<sup>1,8,13,19,47,48</sup> we restrict ourselves to two quantities which are obtained by integration of the LSD and have already been successfully used in Refs. 8 and 49, namely

$$\alpha_P = \int_0^{s_0} P(s) ds \quad (7)$$

and second

$$\alpha_I = \frac{1}{s_0} \int_0^{s_0} I(s) ds, \quad (8)$$

with  $I(s) = \int_0^s P(s') ds'$ . The integration limit is chosen as  $s_0 = 1.4$  which approximates the common crossing point<sup>8</sup> of all LSD curves as can be seen in Fig. 7. Thus  $P(s_0)$  is independent of the distance  $|z_0 - z_c|$  to the critical point and the system size  $N$ . We note that  $N$  is directly related to the RG step  $n$  by  $N = 2^n$ . The double integration in  $\alpha_I$  is numerically advantageous since fluctuations in  $P(s)$  are smoothed. We now apply the finite-size-scaling approach from Eq. (6)

$$\alpha_{I,P}(N, z_0) = f\left(\frac{N}{\xi_\infty(z_0)}\right). \quad (9)$$

Since  $\alpha_{I,P}(N, z_0)$  is analytical for finite  $N$ , one can expand the scaling function  $f$  at the critical point. The first order approximation yields

$$\alpha(N, z_0) \approx \alpha(N, z_c) + a|z_0 - z_c|N^{1/\nu} \quad (10)$$

where  $a$  is a dimensionless coefficient. For our calculation we use a higher order expansion proposed by Slevin and Ohtsuki.<sup>50</sup> In Ref. 50 the function  $f$  is expanded twice, first, in terms of the Chebyshev polynomials of order  $\mathcal{O}_\nu$  and, second, in Taylor series with terms  $|z_0 - z_c|$  in the power  $\mathcal{O}_z$ . This procedure allows to describe the deviations from linearity in  $|z_0 - z_c|$  at the transition. In addition, in Ref. 50 the contributions from an irrelevant scaling variable which leads to a shift of the transition for small system sizes was taken into account. In our case, in contrast to the Anderson model of localization, the transition point  $z_0 = 0$  is known. Therefore, we can neglect the influence of irrelevant variables. In order to

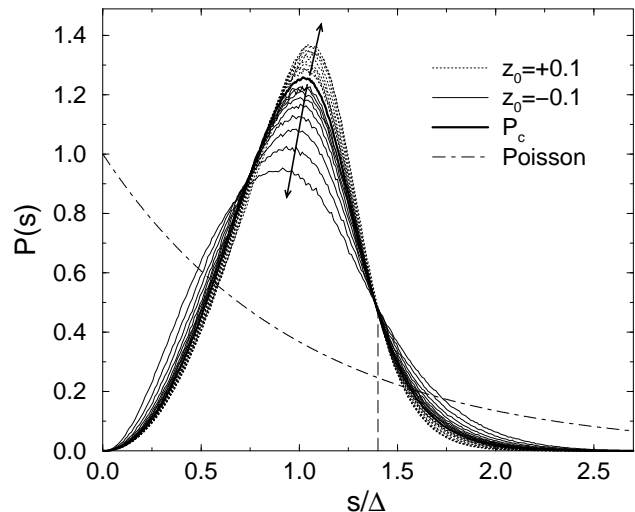


FIG. 7: RG of the LSD used for the computation of  $\nu$ . The dotted lines corresponds to the first 9 RG iterations with an initial distribution  $P_0$  shifted to complete transmission ( $z_0 = 0.1$ ) while the long-dashed lines represent results for a shift toward complete reflection ( $z_0 = -0.1$ ). Within the RG procedure the LSD moves away from the FP as indicated by the arrows. At  $s/\Delta \approx 1.4$  the curves cross at the same point – a feature we exploit when deriving a scaling quantity from the LSD.

obtain the functional form of  $f$ , the fitting parameters, including  $\nu$ , are evaluated by a nonlinear least-square ( $\chi^2$ ) minimization. In Fig. 8 we show the resulting fit for  $\alpha_P$  and  $\alpha_I$  at the transition.

The fits are chosen in such a way that the total number of parameters is kept at a minimal value, while the fit agrees well with the numerical data.<sup>51</sup> The corresponding scaling curves are displayed in Fig. 9. In the plots the two branches corresponding to complete reflection ( $z_0 < 0$ ) and complete transmission ( $z_0 > 0$ ) can be clearly distinguished. In order to estimate the error of fitting procedure we compare the results for  $\nu$  obtained by different orders  $\mathcal{O}_\nu$  and  $\mathcal{O}_z$  of the expansion, system sizes  $N$ , and regions around the transition. A part of our over 100 fit results together with the standard deviation of the fit are given in Table I. The value of  $\nu$  is calculated as the average of all individual fits where the resulting error of  $\nu$  was smaller than 0.02. The error is then determined as the standard deviation of the contributing values. By this method we assure that our result is not influenced by local minima of the nonlinear fit. So we consider  $\nu = 2.37 \pm 0.02$  as a reliable value for the exponent of the localization length at the QH transition obtained from the RG approach to LSD. This is in excellent agreement with  $\nu = 2.35 \pm 0.03$  (Ref. 25),  $2.4 \pm 0.2$  (Ref. 27),  $2.5 \pm 0.5$  (Ref. 29), and  $2.39 \pm 0.01$  (Ref. 32) calculated previously. In addition to  $\alpha_P$  and  $\alpha_I$ , we tested also a parameter-free scaling quantity  $\int_0^\infty s^2 P(s) ds$ ,<sup>47</sup> where the whole distribution  $P(s)$  is taken into account. Here, due to the influence of the large  $s$ -tail a less reliable value

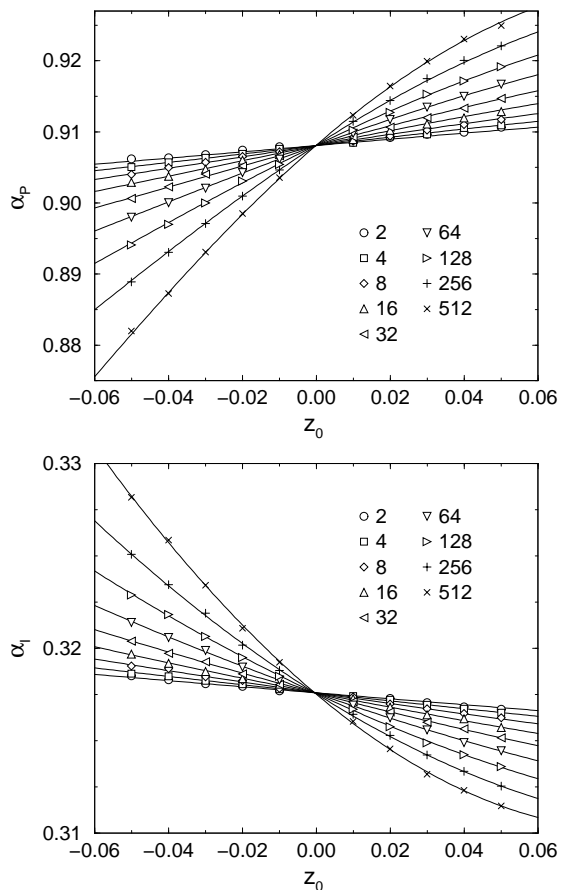


FIG. 8: Behavior of  $\alpha_I$  and  $\alpha_P$  at the QH transition as results of the RG of the LSD. Data are shown for RG iterations  $n = 1, \dots, 9$  corresponding to effective system sizes  $N = 2^n = 2, \dots, 512$ . Full lines indicate the functional dependence according to FSS using the  $\chi^2$  minimization with  $\mathcal{O}_\nu = 2$  and  $\mathcal{O}_z = 3$ .

$\nu = 2.33 \pm 0.05$  was obtained.

### C. Test of consistency

Finally we address the question, how the actual form of the distribution  $Q(z)$  affects the results for LSD and the scaling analysis. Recall that in the above calculations we have used at each step of the RG procedure the distribution  $Q(z)$  derived from the critical conductance distribution,  $P_c(G)$ . The function  $P_c(G)$  is shown in Fig. 10 (inset) with a full line. In order to understand the importance of the fact that  $P_c(G)$  is almost flat, we have repeated our calculations choosing for  $P(G)$  a relatively narrow gaussian distribution  $P(G) \equiv P_{\text{Gau\ss}}(G)$  at each RG step. This distribution is shown with a dashed line in Fig. 10 (inset). The obtained LSD is presented in Fig. 10. Obviously, it agrees much worse with GUE, which can be considered as a reference point, than the LSD computed using the true  $P_c(G)$ . Our data for  $\alpha_I$  calculated for

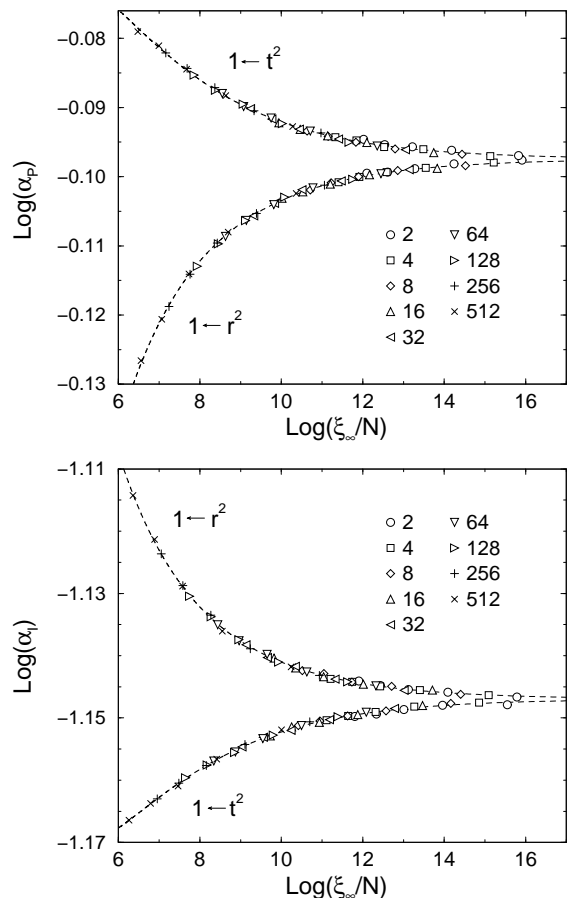


FIG. 9: Finite size scaling curves resulting from the  $\chi^2$  fit of our data shown in Fig. 8. Different symbols correspond to different effective system sizes  $N = 2^n$ . The data points collapse onto a single curve indicating the validity of the scaling approach.

$P(G) = P_{\text{Gau\ss}}(G)$  is plotted in Fig. 11. The curves for small system sizes  $N$  exhibit strong deviations, i.e., there is initially no common crossing point, while for large  $N$  a behavior similar to Fig. 8 is observed. Therefore, small  $N$  data are neglected in the scaling analysis. The  $\chi^2$  fits for  $\alpha_I$  and  $\alpha_P$  are carried out using  $z_0 \in [-0.05, 0.05]$  and  $N = 16 - 512$ . They yield the values  $\nu_I = 2.43 \pm 0.02$  and  $\nu_P = 2.46 \pm 0.03$ , which are also less accurate than  $\nu$  calculated with the critical  $P_c(G)$ . Overall, Figs. 10 and 11 illustrate the consistency of the RG approaches for the conduction distribution and for the level statistics, in the sense, that the best fixed point distribution of the level spacings corresponds to the fixed point of the conductance distribution.

## V. CONCLUSION

Network models introduced in Ref. 52 turned out to be a powerful tool to study the Anderson localization. Without magnetic field, the propagation of electron waves



TABLE I: Part of fit results for  $\nu$  obtained from  $\alpha_I$  and  $\alpha_P$  for different system sizes  $N$ , intervals around the transition, orders  $\mathcal{O}_\nu$  and  $\mathcal{O}_z$  of the fitting procedure.

$N$	$[z_{0\min}, z_{0\max}]$	$\mathcal{O}_\nu$	$\mathcal{O}_z$	$\nu$
$\alpha_P$				
2 – 512	[9.93, 10.07]	3	2	$2.336 \pm 0.010$
2 – 256	[9.93, 10.07]	2	3	$2.412 \pm 0.013$
4 – 512	[9.95, 10.05]	3	1	$2.325 \pm 0.014$
2 – 512	[9.95, 10.05]	2	1	$2.402 \pm 0.014$
2 – 256	[9.95, 10.05]	2	2	$2.360 \pm 0.016$
16 – 512	[9.95, 10.05]	2	3	$2.385 \pm 0.018$
2 – 128	[9.93, 10.07]	1	3	$2.384 \pm 0.019$
4 – 512	[9.93, 10.07]	2	1	$2.471 \pm 0.019$
$\alpha_I$				
2 – 512	[9.93, 10.07]	2	2	$2.383 \pm 0.010$
2 – 512	[9.93, 10.07]	2	3	$2.388 \pm 0.010$
2 – 512	[9.93, 10.07]	3	1	$2.346 \pm 0.012$
8 – 512	[9.93, 10.07]	2	3	$2.376 \pm 0.012$
2 – 512	[9.95, 10.05]	2	3	$2.368 \pm 0.014$
2 – 128	[9.93, 10.07]	2	3	$2.377 \pm 0.016$
16 – 512	[9.95, 10.05]	2	1	$2.367 \pm 0.016$
2 – 256	[9.93, 10.07]	3	3	$2.372 \pm 0.018$

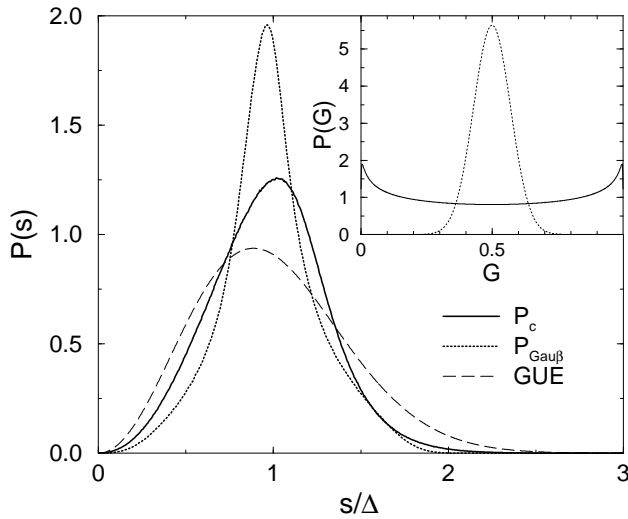


FIG. 10: Comparison of the LSD  $P_c(s)$  and  $P_{\text{Gauß}}(s)$  obtained from the corresponding conductance distributions shown in the inset.

along each link of the network is allowed in both directions. In two dimensions the transmission coefficient of the network is zero for all parameters of the scattering matrix at the nodes,<sup>53</sup> illustrating complete localization of electronic states. On the other hand, the two-channel network model with inter-channel mixing, that models spin-orbit interaction, exhibits a localization-delocalization transition<sup>54</sup> that is also in accord with the scaling theory of localization.<sup>55</sup> However, the version of the network model that has been most widely studied,

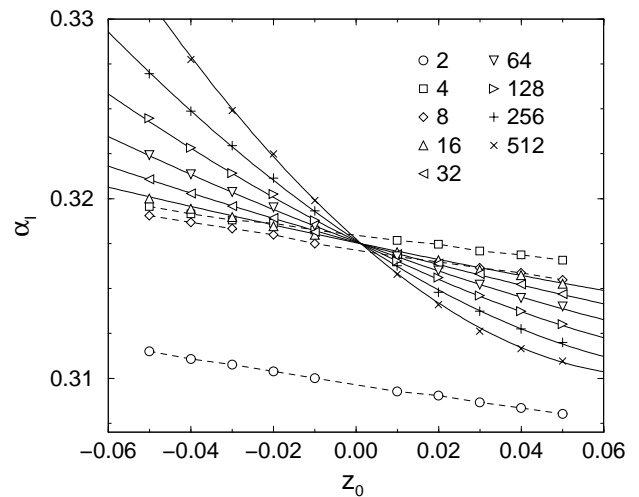


FIG. 11: Behavior of  $\alpha_I$  computed for initial distributions  $P_{\text{Gauß}}$  different from the critical distributions, as shown in Fig. 10. Data are plotted for RG iterations  $n = 1, \dots, 9$  corresponding to effective system sizes  $N = 2^n = 2, \dots, 512$ . Curves for small  $n$  do not cross at the common point  $z_0 = 0$ . Full lines indicate the functional dependence according to FSS using the  $\chi^2$  minimization with  $\mathcal{O}_\nu = 2$  and  $\mathcal{O}_z = 2$ .

is the chiral version, i.e., the CC model,<sup>29</sup> describing the electron motion in a disordered system in a strong magnetic field limit. Within the CC model, the scattering matrix at the node is parametrized by a single number, e.g., the transmission coefficient  $t$ . On the qualitative level, the CC model yields a transparent explanation why delocalization occurs only at a single energy, for which  $t^2 = 1/2$ . On the quantitative level, in addition to the exponent,  $\nu$ , more delicate characteristics of the critical wave functions were extracted from the numerical analysis of the CC model.<sup>56,57</sup>

The fact that the RG approach, within which the correlations between different scales are neglected, describes the results of the large-scale simulations of the CC model so accurately, indicates that only a few spatial correlations within each scale are responsible for the critical characteristics of the quantum Hall transition. More precisely, the structure of the eigenstates of a macroscopic sample at the transition can be predicted from the analysis of a single RG unit consisting of only five nodes. Earlier we have demonstrated this fact for the conductance distribution.<sup>32</sup> In the present paper this statement is reinforced by the study of the level statistics at the transition, which is a complementary (to the conductance distribution) characteristics of the localization.

### Acknowledgments

We thank R. Klesse, L. Schweitzer and I. Zharekeshev for stimulating discussions. This work was supported by the NSF-DAAD collaborative research Grant No. INT-

0003710. P.C. and R.A.R. also gratefully acknowledge the support of DFG within the Schwerpunktprogramm

“Quanten-Hall-Systeme” and the SFB 393.

- 
- \* Permanent address: Department of Physics, University of Warwick, Coventry CV4 7AL, UK, Email: r.roemer@warwick.ac.uk
- <sup>1</sup> B. I. Shklovskii, B. Shapiro, B. R. Sears, P. Lambrianides, and H. B. Shore, Phys. Rev. B **47**, 11487 (1993).
  - <sup>2</sup> J.-L. Pichard and G. Sarma, J. Phys. C **14**, L127 (1981).
  - <sup>3</sup> J.-L. Pichard and G. Sarma, J. Phys. C **14**, L617 (1981).
  - <sup>4</sup> A. MacKinnon and B. Kramer, Phys. Rev. Lett. **47**, 1546 (1981).
  - <sup>5</sup> A. MacKinnon and B. Kramer, Z. Phys. B **53**, 1 (1983).
  - <sup>6</sup> R. Landauer, Phil. Mag. **21**, 863 (1970).
  - <sup>7</sup> D. S. Fisher and P. A. Lee, Phys. Rev. B **23**, 6851 (1981).
  - <sup>8</sup> E. Hofstetter and M. Schreiber, Phys. Rev. B **49**, 14726 (1994).
  - <sup>9</sup> S. N. Evangelou, Phys. Rev. B **49**, 16805 (1994).
  - <sup>10</sup> I. Varga, E. Hofstetter, M. Schreiber, and J. Pipek, Phys. Rev. B **52**, 7783 (1995).
  - <sup>11</sup> T. Kawarabayashi, T. Ohtsuki, K. Slevin, and Y. Ono, Phys. Rev. Lett. **77**, 3593 (1996).
  - <sup>12</sup> M. Batsch, L. Schweitzer, I. K. Zharekeshev, and B. Kramer, Phys. Rev. Lett. **77**, 1552 (1996).
  - <sup>13</sup> I. K. Zharekeshev and B. Kramer, Phys. Rev. Lett. **79**, 717 (1997).
  - <sup>14</sup> M. Metzler, J. Phys. Soc. Japan **67**, 4006 (1998).
  - <sup>15</sup> S. N. Evangelou, Phys. Rev. Lett. **75**, 2550 (1995).
  - <sup>16</sup> L. Schweitzer and I. K. Zharekeshev, J. Phys.: Condens. Matter **7**, L377 (1995).
  - <sup>17</sup> M. Feingold, Y. Avishai, and R. Berkovits, Phys. Rev. B **52**, 8400 (1995).
  - <sup>18</sup> T. Ohtsuki and Y. Ono, J. Phys. Soc. Japan **64**, 4088 (1995).
  - <sup>19</sup> M. Batsch and L. Schweitzer, in *High Magnetic Fields in Physics of Semiconductors II: Proceedings of the International Conference, Würzburg 1996*, edited by G. Landwehr and W. Ossau (World Scientific Publishers Co., Singapore, 1997), pp. 47–50.
  - <sup>20</sup> M. Metzler and I. Varga, J. Phys. Soc. Japan **67**, 1856 (1998).
  - <sup>21</sup> M. Batsch, L. Schweitzer, and B. Kramer, Physica B **249**, 792 (1998).
  - <sup>22</sup> M. Metzler, J. Phys. Soc. Japan **68**, 144 (1999).
  - <sup>23</sup> V. E. Kravtsov, I. V. Lerner, B. L. Altshuler, and A. G. Aronov, Phys. Rev. Lett. **72**, 888 (1994).
  - <sup>24</sup> B. Huckestein and B. Kramer, Phys. Rev. Lett. **64**, 1437 (1990).
  - <sup>25</sup> B. Huckestein, Europhys. Lett. **20**, 451 (1992).
  - <sup>26</sup> B. Huckestein, Rev. Mod. Phys. **67**, 357 (1995).
  - <sup>27</sup> D.-H. Lee, Z. Wang, and S. Kivelson, Phys. Rev. Lett. **70**, 4130 (1993).
  - <sup>28</sup> D. Stauffer and A. Aharony, *Introduction to Percolation Theory* (Taylor and Francis, London, 1992).
  - <sup>29</sup> J. T. Chalker and P. D. Coddington, J. Phys.: Condens. Matter **21**, 2665 (1988).
  - <sup>30</sup> A. G. Galstyan and M. E. Raikh, Phys. Rev. B **56**, 1422 (1997).
  - <sup>31</sup> D. P. Arovas, M. Janssen, and B. Shapiro, Phys. Rev. B **56**, 4751 (1997).
  - <sup>32</sup> P. Cain, R. A. Römer, M. Schreiber, and M. E. Raikh, Phys. Rev. B **64**, 235326 (2001).
  - <sup>33</sup> A. Weymer and M. Janssen, Ann. Phys. (Leipzig) **7**, 159 (1998).
  - <sup>34</sup> M. Janssen, R. Merkt, J. Meyer, and A. Weymer, Physica **256–258**, 65 (1998).
  - <sup>35</sup> Z. Wang, B. Jovanovic, and D.-H. Lee, Phys. Rev. Lett. **77**, 4426 (1996).
  - <sup>36</sup> X. Wang, Q. Li, and C. M. Soukoulis, Phys. Rev. B **58**, 3576 (1998).
  - <sup>37</sup> Y. Avishai, Y. Band, and D. Brown, Phys. Rev. B **60**, 8992 (1999).
  - <sup>38</sup> Y. Ono, T. Ohtsuki, and B. Kramer, J. Phys. Soc. Japan **65**, 1734 (1996).
  - <sup>39</sup> R. Klesse and M. Metzler, Phys. Rev. Lett. **79**, 721 (1997).
  - <sup>40</sup> M. L. Mehta, *Random Matrices* (Academic Press, Boston, 1990).
  - <sup>41</sup> In a “full” RG approach the distributions  $P(t)$  and  $P(s)$  should be iterated simultaneously, which is possible but has proven to be numerically less stable. Therefore  $P_c(t)$  is used in all RG steps without affecting the results. We also note that the chosen form of  $P_0(s)$  does not change  $P_c(s)$  but might alter the speed of convergence.
  - <sup>42</sup> F. Haake, *Quantum Signatures of Chaos*, 2nd ed. (Springer, Berlin, 1992).
  - <sup>43</sup> H. Potempa and L. Schweitzer, J. Phys.: Condens. Matter **10**, L431 (1998).
  - <sup>44</sup> D. Braun, G. Montambaux, and M. Pascaud, Phys. Rev. Lett. **81**, 1062 (1998).
  - <sup>45</sup> L. Schweitzer and H. Potempa, Physica A **266**, 486 (1998).
  - <sup>46</sup> Y. V. Fyodorov and A. D. Mirlin, Phys. Rev. B **55**, 16001 (1997).
  - <sup>47</sup> I. K. Zharekeshev and B. Kramer, Jpn. J. Appl. Phys. **34**, 4361 (1995).
  - <sup>48</sup> I. K. Zharekeshev and B. Kramer, Phys. Rev. B **51**, 17239 (1995).
  - <sup>49</sup> E. Hofstetter and M. Schreiber, Phys. Rev. B **48**, 16979 (1993).
  - <sup>50</sup> K. Slevin and T. Ohtsuki, Phys. Rev. Lett. **82**, 382 (1999).
  - <sup>51</sup> M. L. Ndawana, R. A. Römer, and M. Schreiber, Eur. Phys. J. B **27**, 399 (2002).
  - <sup>52</sup> B. Shapiro, Phys. Rev. Lett. **48**, 823 (1982).
  - <sup>53</sup> P. Freche, M. Janssen, and R. Merkt, Phys. Rev. Lett. **82**, 149 (1999).
  - <sup>54</sup> R. Merkt, M. Janssen, and B. Huckestein, Phys. Rev. B **58**, 4394 (1998).
  - <sup>55</sup> S. Hikami, A. I. Larkin, and Y. Nagaoka, Prog. Theor. Phys. **63**, 707 (1980).
  - <sup>56</sup> B. Huckestein and R. Klesse, Phys. Rev. B **59**, 9714 (1999).
  - <sup>57</sup> R. Klesse and M. R. Zirnbauer, Phys. Rev. Lett. **86**, 2094 (2001).